Desalination and Water Treatment
www.deswater.com

doi: 10.5004/dwt.2019.23737

151 (2019) 219–229
May

Preparation of formaldehyde-free persimmon tannin-based rigid foam as an adsorbent for selective recovery of Au(III) ions

Ruiyi Fan[a,b], Xingxing Hong[b], Huiyu Min[b], Qingping Yi[c], Qinglin Zhang[b,d], Zhengrong Luo[b,d,*]

[a] *Institute of Fruit Tree Research, Guangdong Academy of Agricultural Sciences, Key Laboratory of South Subtropical Fruit Biology and Genetic Resource Utilization (MOA); Guangdong Province Key Laboratary of Tropical and Subtropical Fruit Tree Research, Guangzhou, 510640, China, email: fanruiyi@outlook.com (R. Fan)*
[b] *Key Laboratory of Horticultural Plant Biology (MOE), Huazhong Agricultural University, Wuhan 430070, China*
[c] *College of Bioengineering, Jingchu University of Technology, Jingmen 448000, China*
[d] *Hubei Collaborative Innovation Center for the Characteristic Resources Exploitation of Dabie Mountains, Huanggang Normal University, Huanggang 438000, China, email: luozhr@mail.hzau.edu.cn (Z. Luo)*

Received 19 August 2018; Accepted 29 December 2018

ABSTRACT

A new and green tannin rigid foam was prepared without using formaldehyde and named as "Kaki-TRF" since the tannin is derived from waste persimmon (*Diospyros kaki* Thunb.) barks. Persimmon tannin is highly reactive and the cross linker is not necessary. The prepared foam was of porous nature and the Brunauer-Emmett-Teller (BET) surface area is 7.014 $m^2 g^{-1}$. Adsorption of Au(III) ions from aqueous solution by Kaki-TRF was investigated including the effect of solid-liquid ratio, initial pH, reaction time, initial concentration of Au(III) and ionic strength. The selective property of Kaki-TRF toward Au(III) was examined in both static and continuous adsorption manners. Pseudo-second-order and Langmuir can well fit the experimental data of adsorption kinetics and isotherms. The calculated maximum adsorption capacity of Kaki-TRF toward Au(III) is 1.31 mmol g^{-1} which is relatively high compared with other porous bio-sorbents. Electrostatic attraction and in situ reduction were proposed to be the main adsorption mechanisms. The adsorption-regeneration recycling test proved that Kaki-TRF can be reused for at least five times.

Keywords: Persimmon bark; Tannin rigid foam; Adsorption; Au(III); Selective recovery

---

1. Introduction

Gold has been utilized in various fields for its unique physical and chemical properties. The demanding and price of gold is increasing while the stock of primarily gold ore is limited [1]. The process of gold selection from ore results in unavoidably harmful to the geomorphology and ecology nearby [2]. Therefore, recovery of gold from secondary waste solution containing Au(III) is beneficial for environmental benignity and sustainability. Under this circumstance, numbers of literatures concerning gold adsorption and recovery have been published [1]. Adsorbents derived from natural biomass exhibited lots of benefits such as low cost, high and sustainable availability, rich in functional groups, etc.

Condensed tannin is one kind of plant polyphenol containing large amounts of hydroxyl groups and exhibiting favorable reduction capacity toward precious metal ions. Among various tannins, persimmon tannin presented astonished highly Au(III) selective uptake amount [3]. Persimmon (*Diospyros kaki* Thunb., also known as "kaki") is an important fruit tree in China, Korea, Spain Japan, etc., which is necessary to prune the branches in order to maintain the shape of

---

* Corresponding author.

the tree and improve the quality of fruits. After training and pruning, there are huge amounts of branches as agricultural waste waiting for proper disposal in orchard. Persimmon tannin in the barks of these discarded branches should be exploited to make profits for the environment. Nevertheless, there are no adsorbents based on persimmon bark tannin until now. As for other kinds of bark tannin, a majority of them were used for synthesis of bio-resourced foams which is established as Tannin-based Rigid Foams (TRF). TRF have been widely utilized as architectural materials for their inherent low thermal and humid absorption, fire prevention, compression resistance and noise insulation [4–8]. The possible application of TRF in other fields such as agriculture, electronics and environment have been recently exploited, for instance, TRF of different formulations were served as supportive matrices for horticulture and hydroponics [9], semi-conductor [10], electromagnetic shielding [11], heavy metal ions and organic pollutants adsorbents [12,13]. The raw material and reagents used during the preparation of typical TRF includes tannins, the cross linkers also known as the hardeners, blowing agents and catalysts. The condensed tannin in TRF was mainly derived from mimosa (*Acacia mearnsii*), pine (*Pinus radiata*), Quebracho (*Schinopsis* sp.), maritime pine (*Pinus pinaster*) and Norway spruce (*Picea abies* L.). Notably, mimosa was firstly used in 1994 and is also frequently applied until now, while the first pine tannin foam was prepared in 2013 [14]. Principally, the monomers of mimosa and quebracho tannin are robinetinidin and fisetinidin, respectively. In general, their reaction activity is less than that of the procyanidin-type pine. The high reactivity of pine tannins is tricky during synthesis since the foaming procedure should be coordinated with resin hardening [14]. The monomers of persimmon tannin are of both cyanidin and delphinidin form with myricetin terminal unit. Persimmon tannin is highly galloylated which means its hydroxyl content is much higher. The interflavan linkage of persimmon tannin is a mixture of B-type and A-type [15]. Hence, it can be inferred that the reaction activity of persimmon tannin is higher than that of pine tannins. All of these special characters existing in persimmon tannin produce both advantages and challenges to prepare a different TRF as a new adsorbent for gold recovery.

In this research, persimmon (kaki) tannin-based rigid foam (Kaki-TRF) was prepared for the first time, and the toxic hardener, formaldehyde, was avoided during preparation. The adsorption parameters including dosage, initial pH, reaction time and initial concentration of Au(III) was optimized in single-ion system. Adsorption behavior of Kaki-TRF toward Au(III) from multiply-ions system was examined to judge the selectivity of Kaki-TRF. Finally, preparation and structure of Kaki-TRF were characterized and adsorption mechanisms were proposed. Kaki-TRF is a new and green porous material with high adsorption capacity for selective recovery of Au(III).

2. Experimental setup

2.1. Materials and chemicals

Persimmon or kaki (*Diospyros kaki* Thunb.) barks were collected after winter pruning from the Persimmon Repository of Huazhong Agricultural University, Wuhan, China. The barks were firstly washed with distilled water, dried at room temperature, ground and sieved to 30 mesh then kept in sealed bottle. Furfuryl alcohol and pentane were purchased from Macklin Biochemical Co. Ltd., Shanghai, China. Polyethylene glycol, para-toluene-4-sulfonic acid (pTSA), $HAuCl_4{\cdot}4H_2O$, NaOH, HCl, NaCl, KCl, $MgCl_2{\cdot}6H_2O$, $CaCl_2$, $NiCl_2{\cdot}6H_2O$, $MnCl_2{\cdot}4H_2O$, $CuCl_2{\cdot}4H_2O$, $CoCl_2{\cdot}6H_2O$ and $Pb(NO_3)_2$ were purchased from Sinopharm Chemical Reagent Co. Ltd., Beijing, China. Deionized water was used for all the experiments. All the chemicals and reagents were utilized as received.

2.2. Instrumentation

Atomic absorption spectrophotometer (Varian Spectra AA 220) was applied to measure the concentrations of metal ions. Elemental analysis was conducted by Elementar (Vario EL cube). Nitrogen adsorption-desorption isotherms were obtained at −196°C with a Micromeritics apparatus (TriStarII 3020). Brunauer-Emmett-Teller (BET) surface area of Kaki-TRF was calculated from the BET plot. Surface morphology of Kaki-TRF before and after adsorption was observed by SEM-EDS (JSM-5610LV). XRD patterns of Kaki-TRF before and after adsorption were recorded on a Bruker D8 advance diffractometer. The Fourier transform infrared spectroscopy (FTIR) spectra of Kaki-TRF and Au(III)-loaded Kaki-TRF were recorded by Thermo Nicolet Nexus spectrophotometer by KBr pellet method. The XPS spectra of Kaki-TRF and Au(III)-loaded Kaki-TRF were obtained by ESCALAB 250Xi (Thermo Fisher), and the spectra were analyzed by Avantage 5.52.

2.3. Preparation of Kaki-TRF

Persimmon tannin-based rigid foam was prepared according to the method proposed previously [14] with some modification. First, a solution of 11.67 g of furfuryl alcohol, 0.3 g of polyethylene glycol and 0.4–0.6 g of pentane was prepared and mixed vigorously for 10 s. Then 3.5 g of persimmon bark powder was added into the liquid mixture and stirred rigorously for 90 s. Finally, 5.2 g of 65% (wt%) pTSA water solution was added to the above mixture and stirred. The foaming initiated several seconds after the catalyst was added and terminated in 30 s. The curing was allowed in the chemical hood at room temperature for 24 h. Before utilization for adsorption experiments, Kaki-TRF was washed with deionized water thoroughly to remove the entire unreacted compound, dried overnight in the furnace at 65°C, ground and sieved to 60 mesh.

2.4. Adsorption experiments

2.4.1. Batch static adsorption

The specific adsorption procedure was similar with previous work [16]. The adsorbent dosage of 0.50, 0.75, 1, 1.25, 1.50, 2.00, 2.50 g L^{-1} was employed to 1 mmol L^{-1} Au(III)-solution for 24 h to examine the effect of solid/liquid ratio. The pH of Au(III)-solution with initial concentration of 1 mmol L^{-1} was adjusted to 1.0–6.0 in the test of initial pH effect. For kinetics study, 1 mmol L^{-1} of Au(III)-solution was reacted with Kaki-TRF in varied time (5–1,440 min). Different initial Au(III) concentrations (0.76–6.00 mmol L^{-1}) were applied to get the maximum adsorption amount. A mixture solution containing coexisting metal ions of Au(III), K(I), Ca(II), Na(I), Mg(II), Cu(II), Pb(II), Mn(II), Co(II) and Ni(II) (the conc. of single metal ion is 1 mmol L^{-1}) was employed to examine the effect of interfering metal ions on the adsorption capacity of TRF toward Au(III). The adsorption capacity (q_e) and adsorption rate (%Adsorption) were calculated through the following equations:

$$q_e = \frac{(C_i - C_e)V}{m} \tag{1}$$

$$\%\,\text{Adsorption} = \frac{C_i - C_e}{C_i} \times 100 \tag{2}$$

where C_i (mg L^{-1}) and C_e (mg L^{-1}) are the initial and equilibrium concentration of Au(III) in solution, respectively, m (g) is the weight of Kaki-TRF and V (L) is the volume of Au(III)-solution.

2.4.2. Dynamic column adsorption

A dynamic column experiment was conducted in a mimic industrial adsorption column with the internal diameter of 1 cm and the height of 15 cm. A constant flow pump (DHL-A) and an automatic fraction collector (BSA-100) was equipped with the adsorption column to keep flow rate and monitor the concentration of metal ions in effluents.

The specific operation was carried out according to our previous report [16] with some minor modification. First, 400 mg Kaki-TRF was immersed in deionized water overnight before being added into the column. Secondly, deionized water was used to wash the column for 24 h at a flow rate of 3.0 mL min^{-1}. Finally, Au(III)-solution containing coexisting metal ions (the conc. of Au(III), K(I), Ca(II), Na(I), Mg(II), Cu(II), Pb(II), Mn(II), Co(II) and Ni(II) is 1 mmol L^{-1}) was pumped through the column at a constant flow rate of 6.0 mL h^{-1}. The automatic fraction collector was set to gather effluent samples hourly. In column adsorption, bed volume (*B.V.*) is always employed to evaluate the efficiency of adsorption and is defined as:

$$B \cdot V \cdot = \frac{vt}{V} \tag{3}$$

where v (mL h^{-1}) is the flow rate, t (h) is the conducting time, and V (mL) is the volume of adsorbent packed in the column.

3. Results and discussion

3.1. Optimization of the adsorption process in single-ion system

3.1.1. Effect of dosage

The effect of dosage exerts influence on both adsorption capacity and rate. The results illustrated in Fig. 1(a) indicated

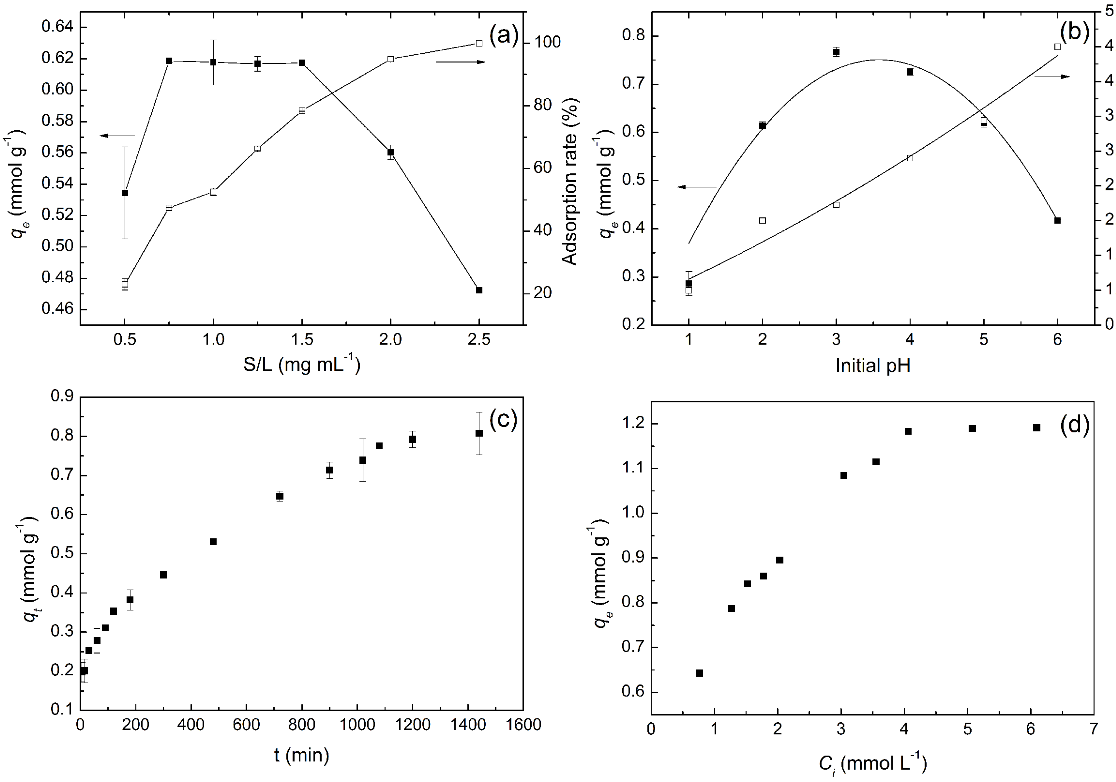

Fig. 1. Effects of solid/liquid ratio (a), initial pH (b), reaction time (c) and initial concentration of Au(III) (d) on adsorption capacity. (q_e: equilibrium adsorption amount; C_i: initial concentration of Au(III); q_t: adsorption amount at time t).

that with the increasing of dosage, the adsorption capacity firstly increased then decreased, however, the adsorption rate showed a positive relationship with the dosage. It is obvious that adsorption rate is only determined by the decreasing of metal ions in the adsorption system so that with the increasing usage of Kaki-TRF, more auric ions will be adsorbed. As for adsorption capacity, it is determined by the ratio of adsorbed ions to the usage of the adsorbents. Decrement of adsorption capacity in higher dosage owns the limited auric ions which could not catch up with the increment of binding sites on Kaki-TRF. Dosage of 0.75 mg mL^{-1} was applied to the following tests except special declaration.

3.1.2. Effect of initial pH

From Fig. 1(b), it is obvious that the maximum adsorption capacity of Kaki-TRF reaches at pH 3.0. In the pH below 3.0, $AuCl_4^-$ is the main complex of Au(III). The pH_{pzc} of Kaki-TRF was determined to be 3.7, so the surface charge of Kaki-TRF is positive at pH lower than 3.7, which is favorable for adsorption owning to the electrostatic affinity between the negative charged gold complex and Kaki-TRF. However, the decreasing of adsorption capacity is attributed to the suppression of the ionization of phenolic hydroxyls at low pH range of 2.0–3.0 [17]. The adsorption capacity of Kaki-TRF also decreased when pH is higher than 3.0 because of the repellent force between negative charged Kaki-TRF and gold complex like $AuCl_4^-$ and $AuCl_3(OH)^-$. The pH was also measured after the equilibrium of adsorption which was illustrated in Fig. 1(b). The decrease of pH might be the release of H^+ after the oxidation of hydrogen groups on Kaki-TRF. Initial pH of 3.0 was applied to the following tests except special declaration.

3.1.3. Adsorption kinetics

To explore the effect of reaction time, 1 mmol L^{-1} Au(III) was applied under a time range of 5–2,880 min and the experimental data are presented in Fig. 1(c). It can be seen half of Au(III) was adsorbed sharply during initial 200 min and adsorption amount increased gradually with the prolonged contact time from 200 to 1,200 min. It means that two phases occurred in the Au(III) adsorption process. Different adsorption mechanisms were involved in the gold uptake, which might be electrostatic attraction and redox. The maximum adsorption capacity of Kaki-TRF was obtained at 1,200 min. Reaction time of 1,200 min was applied to the following tests except special declaration.

To reveal the adsorption kinetic mechanism, Pseudo-first-order, Pseudo-second-order, Intraparticle diffusion and Elovich were used to fit the experimental data of adsorption kinetics by linear fitting. The definition and explanation of these models were described in Supplementary Material. The results of fitting are illustrated in Fig. S1. The parameters calculated from the equations were presented in Table 1. Adsorption kinetics could be well described by intraparticle diffusion and pseudo-second-order model according to the higher correlation coefficient ($R^2 > 0.97$). In addition, the theoretic adsorption capacity of 0.85 mmol g^{-1} was very close to the value obtained from the experiment (Table 1). The fitting line of intraparticle diffusion model (Fig. S1(c)) did not pass through the origin ($C \neq 0$) which indicated that the adsorption was controlled by hybrid phases rather than internal diffusion [18].

3.1.4. Adsorption isotherms

Effect of different initial Au(III) concentration was explored to obtain the maximum adsorption capacity at room temperature. As shown in Fig. 1(d), the adsorption capacity of Kaki-TRF increased with the increment of initial Au(III) concentration and finally reached a highest value of 1.19 mmol g^{-1}. Freundlich, Langmuir and Temkin models were applied to fit the experimental data of Au(III) adsorption isotherm onto Kaki-TRF. Details about these models were provided in Supplementary Material. The fitting plots of experimental data are illustrated in Fig. S2 and calculated parameters are shown in Table 2. Au(III) adsorption isotherm onto Kaki-TRF could be best described by Langmuir according to the highest correlation coefficient ($R^2 = 0.9955$). The maximum adsorption capacity was 1.31 mmol g^{-1} which is relatively high compared with other porous bio-based adsorbents (Table 3). When a comparison is made, the temperature is very important to consider owning to the proposed adsorption mechanism of oxidation and reduction. The correlation

Table 2
Langmuir, Freundlich and Temkin parameters for Au(III) adsorption on Kaki-TRF

Langmuir		Freundlich		Temkin	
q_m (mmol g^{-1})	1.31	K_F (mmol$^{1-1/n}$ L$^{1/n}$ g^{-1})	0.8620	K_T	62.39
K_L (L mmol^{-1})	2.14	n	4.33	b	293.19
R^2	0.9955	R^2	0.9711	R^2	0.9598

Table 1
Pseudo-first-order, Pseudo-second-order, Intraparticle diffusion and Elovich parameters for Au(III) adsorption on Kaki-TRF

Experimental Q_e (mmol g^{-1})	Pseudo-first-order			Pseudo-second-order		
	$K_1 \times 10^{-3}$ (min^{-1})	R^2	$Q_{e,\mathrm{cal}}$ (mmol g^{-1})	$K_2 \times 10^{-3}$ (g mmol^{-1} min^{-1})	R^2	$Q_{e,\mathrm{cal}}$ (mmol g^{-1})
0.80	3.961	0.6306	0.88	7.983	0.9870	0.85
	Intraparticle diffusion			Elovich		
	$K_{id} \times 10^{-2}$ (mmol g^{-1} min$^{-0.5}$)	R^2	C	K_E	R^2	A
	1.855	0.9937	0.141	0.1229	0.8722	–0.1583

coefficients of Temkin model was poor compared that with Langmuir and Freundlich (Table 2), so Temkin model failed to describe the adsorption process

3.2. Adsorption behavior of Kaki-TRF in multiply-ions system

The industrial gold liquor often contains a variety of metal ions, so a multiply-ions system was applied to Kaki-TRF by both static and continuous adsorption tests in order to explore its potentiality for commercial application. To understand the selectivity of Kaki-TRF, a solution containing both light and heavy metal ions (K^+, Ca^{2+}, Na^+, Mg^{2+}, Cu^{2+}, Pb^{2+}, Mn^{2+}, Co^{2+} and Ni^{2+}) was prepared in the same concentration (1 mmol L^{-1}) and the pH of this solution was maintained as 2 to avoid the precipitation. It is clear in Fig. 2(a) that the selectivity of Kaki-TRF toward Au(III) is very high and the adsorption capacity decreased 2% compared with that in the single-ion system. It is manifested that the disturbing effect of coexisting metal ions is weak. The adsorption amount of Au(III) in different ionic strength (calculated by the concentration of Na^+) ranged from 0.82 to 0.70 mmol g^{-1} (data shown in Fig. S3). In industrial practice, column adsorption is a good choice for resin-type adsorbents. In the present research, a mini-column (compared with the industrial one) was applied to conduct the continuous adsorption test. Fig. 2(b) illustrates the breakthrough profiles of all the metal ions in the multiply-ions system. It is evident that the breakthrough of other coexisting metal ions like K(I), Ca(II), Na(I), Mg(II), Cu(II), Pb(II), Mn(II), Co(II) and Ni(II) took place almost immediately at the beginning of the flow, indicating that there is no affinity between those coexisting metal ions and the Kaki-TRF-column. The breakthrough of Au(III) occurred after 80 *B.V.*, suggesting that Kaki-TRF is able to treat at least 80 times of the solution containing Au(III) and other coexisting metal ions compare with its own volume with high selectivity.

Table 3
Comparison of maximum adsorption capacities of Au(III) by using various porous or bio-based adsorbents

Adsorbents	q_m (mmol g^{-1})	Temperature (K)	References
Hard shell of apricot stones	0.031	298	[19]
Magnetic porous graphitic carbon	0.0378	Room temperature	[20]
Ion exchange polyurethane foams	0.35	298	[21]
Cedar bark powder	0.469	Not mention	[22]
Activated rice husk	0.474	333	[23]
Barley straw porous carbon	0.76	303	[24]
Ligand immobilized mesoporous adsorbent	0.903	298	[25]
MCM mesoporous adsorbents	0.40–1.40	295 ± 2	[26]
Rice husk porous carbon	1.47	303	[24]
Kaki-TRF	1.31	298	Present study

3.3. Characterization of Kaki-TRF and adsorption mechanism

Even though the real chemical structure of persimmon tannin (PT) is not fully understood, it is proven that the basic skeleton of PT is procyanidins and prodelphinidins with the possible esterification of the hydrogen in C_3 with gallic acid. Matsuo and Ito reported that PT belonged to the proanthocyanidin B type with the interflavan linkages between C–4 and C–8 [27]. Li et al., [15] also found A-type interflavan linkages dimer from the purified PT. In general, persimmon tannin is a mixture of both high and low molecular with superior high reactivity. As a result, the dosage of persimmon bark tannin was decreased to control the simultaneous hardening of the

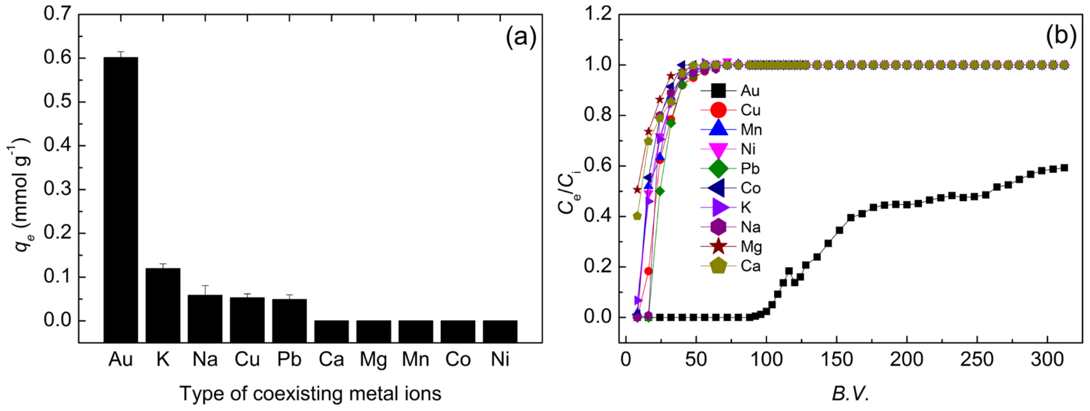

Fig. 2. The interfaces of coexisting metal ions on Au(III) adsorption (a) and breakthrough profile of Au(III) with coexisting metal ions on Kaki-TRF (b). (q_e: adsorption amount; C_e: equilibrium concentration of Au(III); C_i: initial concentration of Au(III)).

rigid foam with reaction exotherm and solvent blowing. The foaming of Kaki-TRF is quite fast that starts merely several seconds after the catalyst was added and terminated in about 30 s. It is quite reasonable owning to the high reactivity of persimmon tannin. Different from the more elastic behavior of pine tannin-based rigid foam without formaldehyde [14], Kaki-TRF is rather crispy and easily ground to powder. The elemental analysis revealed that this new material contains carbon (66.51%), oxygen (27.60%), hydrogen (5.43%), sulfur (0.32%) and nitrogen (0.14 %). And the water adsorption capacity of TRF is 1.63 g/g. Characterization of Kaki-TRF before and after adsorption of Au(III) was examined by SEM-EDS, XRD, FTIR spectra and XPS. From the SEM images presented in Fig. 3 it is clear that this new foam is porous with fairly rough surface produced by the pentane blowing caused by strong heat release. In addition, the BET surface area of Kaki-TRF is measured to be 7.014 $m^2 g^{-1}$. The relatively high surface area of Kaki-TRF is advantageous for industrial application on account of the balance for high adsorption capacity and solid liquid separation. The porous nature of Kaki-TRF also can provide numerous binding sites for Au(III) adsorption. It is worth noting that nano and micro grade metallic gold were observed on the surface of Kaki-TRF as shown in Fig. 3(c), and the EDS spectrum of Kaki-TRF after adsorption (Fig. 3(d)) also proved the existence of Au element.

Wide-angle X-ray diffraction technology was applied to observe the crystalline nature of Kaki-TRF before and after Au(III) adsorption. As presented in Fig. 4, Kaki-TRF had no crystal structure. The peaks of Au(III)-loaded Kaki-TRF at 2θ value of 38.28, 44.50, 64.65 and 77.61 indicated the existence of typical metallic gold which means that auric complex has been reduced during the adsorption.

In the FTIR spectrum of Kaki-TRF (Fig. 5), the characteristic strong broad band's at 3,420 and 3,409 cm^{-1} are attributed to O–H (phenolic hydroxyl groups) stretching vibration, and the weak band at 3,124 and 3,107 cm^{-1} presents the stretching vibration of –C–H and = C–H belonging to benzene ring. The sharp bands at 2,920 and 2,905 cm^{-1} are due to $–CH_2–$ asymmetrical stretching. After adsorption, the decreasing of the intensity of the band 3,409 cm^{-1} assigned for phenolic hydroxyl stretching vibration indicated the oxidation of Kaki-TRF. X-ray photoelectron spectroscopy (XPS) analysis of Kaki-TRF before and after gold adsorption was also conducted to further elucidate the adsorption mechanism. XPS survey and O 1 s spectra of Kaki-TRF and Au(III)-loaded Kaki-TRF are illustrated in Fig. 6. After adsorption, there are new binding energy peaks at 353.70 , 335.86 , 87.86 and 84.15 eV corresponding to Au 4d3/2, Au 4d5/2, Au 4f5/2 and Au 4f7/2 which indicated large amount of gold has been adsorbed on Kaki-TRF. In addition, binding energy peak at 87.86 and 84.15 eV reveals the existence of metallic gold. XPS spectra of O1 s were demonstrated in Figs. 6(c) and (d). Peaks at the binding energy of 533.76 and 532.65 eV is assigned to C–O and –OH which are the main chemical states of oxygen on Kaki-TRF. After adsorption the

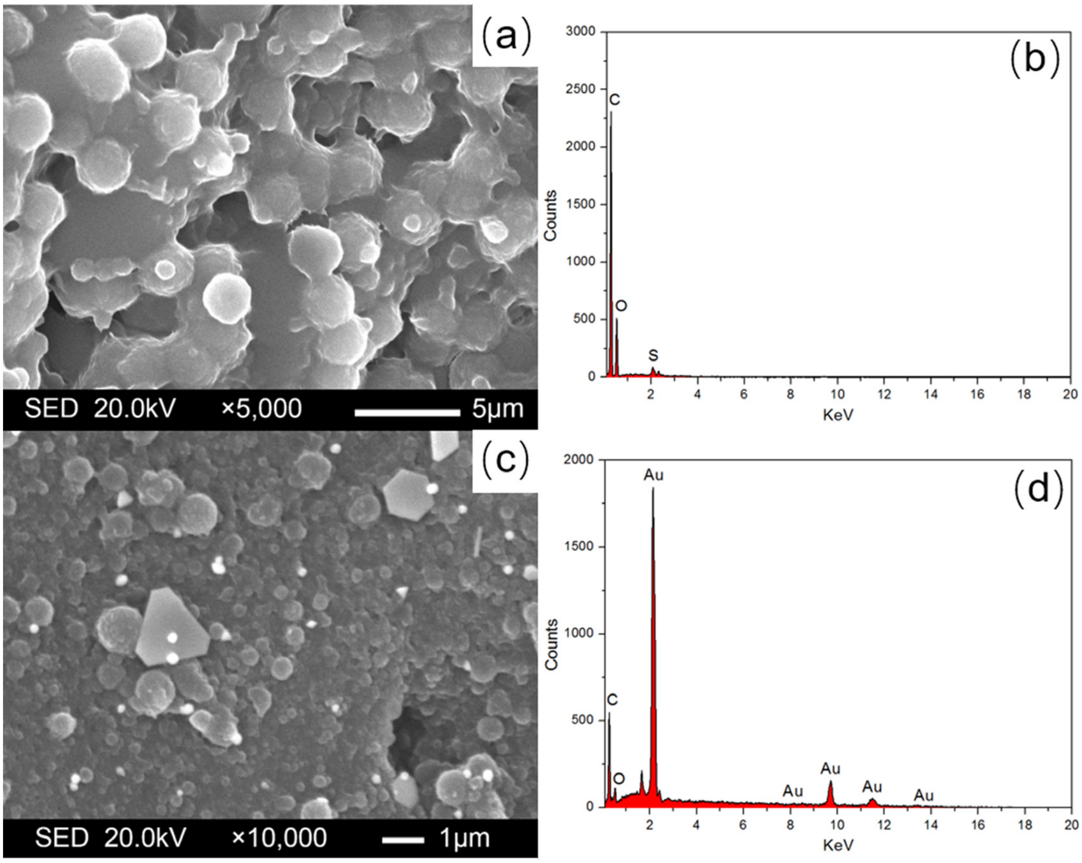

Fig. 3. SEM images of (a) Kaki-TRF, (c) Au(III)-loaded Kaki-TRF, and EDS spectra of (b) Kaki-TRF, (d) Au(III)-loaded Kaki-TRF.

binding energy peak of –OH disappeared with the appearance of a new peak at 534.79 corresponding to C=O bond owning to the oxidation of phenolic hydroxyl group on Kaki-TRF. Based on the combined analysis of XRD, FTIR and XPS, in situ Au(III)-reduction is proposed to be one of the adsorption mechanism. Owning to the pH-dependent nature of Kaki-TRF in different initial pH test, electrostatic attraction also attributes to the adsorption mechanism. Moreover, the results of kinetics and isotherms fitting demonstrated that adsorption process is controlled by hybrid phases and chemisorption is the main adsorption mechanism. In consequence, electrostatic attraction and redox account for the proposed adsorption mechanism of Au(III) onto Kaki-TRF.

3.4. Reusability of Kaki-TRF

The capacity of adsorption and regeneration of adsorbents for recycling utilization is vital for commercialization.

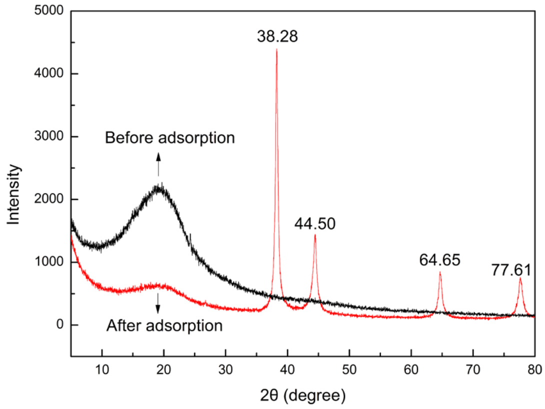

Fig. 4. X-ray diffraction pattern of Kaki-TRF before and after adsorption.

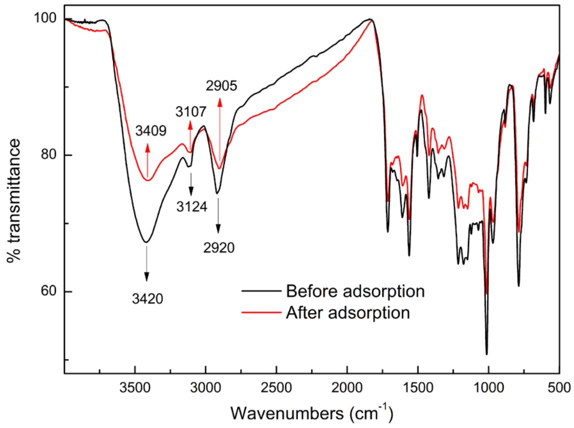

Fig. 5. FTIR spectra of Kaki-TRF before and after adsorption.

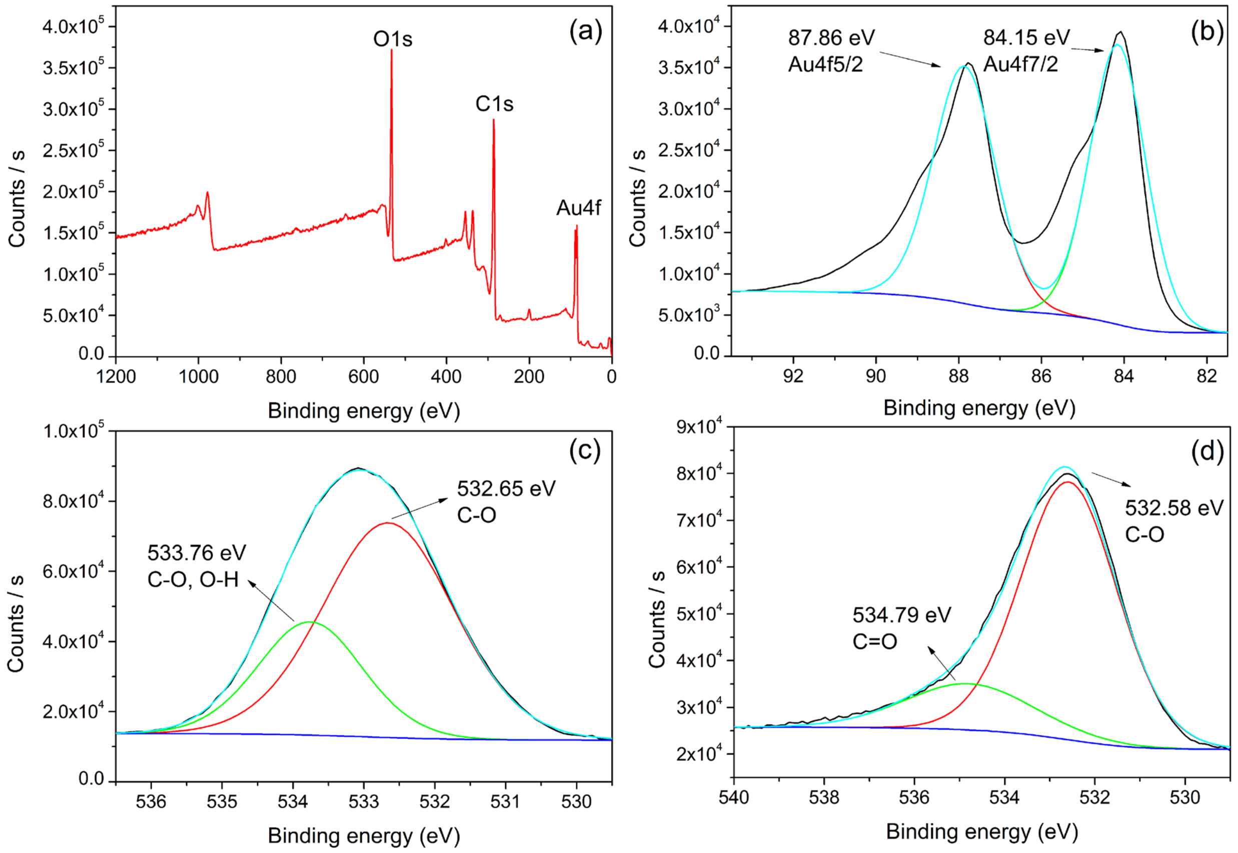

Fig. 6. XPS survey and O 1 s on Kaki-TRF before (a, c) and after (b, d) adsorption.

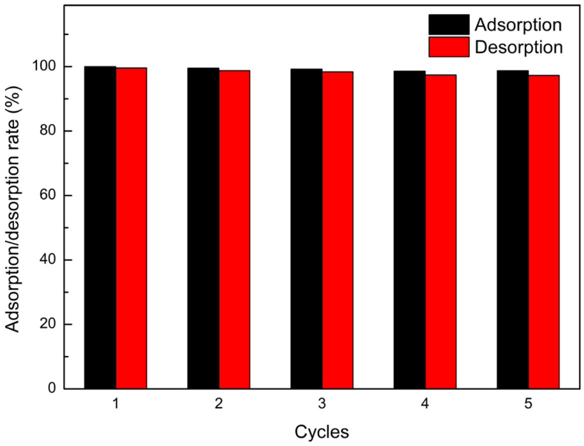

Fig. 7. Rusablity test of Kaki-TRF (regenerated by 0.5 mol L–1 thiourea in 0.5 mol L–1 HCl).

Therefore, an adsorption-desorption-regeneration test is conducted for Kaki-TRF. 0.5 mol L^{-1} thiourea in 0.5 mol L^{-1} HCl and solo 0.5 mol L^{-1} HCl are chosen to elute the adsorbed Au(III) and compare the desorption efficiency. The elution rate of diluted HCl and acidic thiourea are 17.77% and 99.58%, respectively. Hence, acidic thiourea is selected to carry out the reusability test and the recycling results are presented in Fig. 7. The adsorption efficiency shows no significate decrease even after five times of recycling, which indicates a good reusability of Kaki-TRF.

4. Conclusion

Persimmon tannin based rigid foam was successfully prepared without formaldehyde. Kaki-TRF is porous and rich in phenol hydrogen groups due to the highly galloylated nature of persimmon tannin which is in favour of capturing metal ions from aqueous solution. The adsorption process was optimized by studying the effect of dosage, initial pH, reaction time and initial Au(III) concentration. Adsorption kinetics of Au(III) by Kaki-TRF could be fitted by both pseudo-second order and intraparticle diffusion models. Langmuir is the best model to describe the adsorption isotherm, and the calculated maximum adsorption capacity of Kaki-TRF is 1.31 mmol g^{-1} which is relatively high compared with other type of bio-based porous adsorbents. The selectivity of Kaki-TRF toward Au(III) in a mixed solution containing different coexisting metal ions is good in both static and dynamic adsorption tests which indicated that Kaki-TRF could be a promising candidate for application in industrial practice. Electrostatic attraction and redox are the main adsorption mechanism. In addition, Kaki-TRF could be regenerated and reused for at least five times.

Acknowledgements

This research was funded by Hubei Collaborative Innovation Center for the Characteristic Resources Exploitation of Dabie Mountains (2015TD01), Special Fund for Agro-scientific Research in the Public Interest (201203047) and Scientific Research Project of Hubei Provincical Dapartment of Education (D20174302).

References

[1] S. Syed, Recovery of gold from secondary sources—A review, Hydrometallurgy, 115–116 (2012) 30–51.
[2] C. Roussel, C. Neel, H. Bril, Minerals controlling arsenic and lead solubility in an abandoned gold mine tailings, Sci. Total. Environ., 263 (2000) 209–219.
[3] H.A.M. Bacelo, S.C.R. Santos, C.M.S. Botelho, Tannin-based biosorbents for environmental applications – A review, Chem. Eng. J., 303 (2016) 575–587.
[4] C. Delgado-Sánchez, M. Letellier, V. Fierro, H. Chapuis, C. Gérardin, A. Pizzi, Hydrophobisation of tannin-based foams by covalent grafting of silanes, Ind. Crop. Prod., 92 (2016) 116–126.
[5] N. Meikleham, A. Pizzi, Acid and alkali-catalyzed tannin-based rigid foams, J. Appl. Polym. Sci., 53 (1994) 1547–1556.
[6] C. Lacoste, M.C. Basso, A. Pizzi, A. Celzard, E. Ella Ebang, N. Gallon, Pine (*P. pinaster*) and quebracho (*S. lorentzii*) tannin-based foams as green acoustic absorbers, Ind. Crop. Prod., 67 (2015) 70–73.
[7] G. Tondi, W. Zhao, A. Pizzi, G. Du, V. Fierro, A. Celzard, Tannin-based rigid foams: a survey of chemical and physical properties, Bioresour. Technol., 100 (2009) 5162–5169.
[8] G. Tondi, A. Pizzi, Tannin-based rigid foams: characterization and modification, Ind. Crop. Prod., 29 (2009) 356–363.
[9] M.C. Basso, A. Pizzi, F. Al-Marzouki, S. Abdalla, Horticultural/hydroponics and floral natural foams from tannins, Ind. Crop. Prod., 87 (2016) 177–181.
[10] G. Tondi, M. Johansson, S. Leijonmarck, S. Trey, Tannin based foams modified to be semi-conductive: synthesis and characterization, Prog. Org. Coat., 78 (2015) 488–493.
[11] M. Letellier, J. Macutkevic, A. Paddubskaya, A. Plyushch, P. Kuzhir, M. Ivanov, Tannin-based carbon foams for electromagnetic applications, IEEE Trans Electromagn. Compat., 57 (2015) 989–995.
[12] G. Tondi, C.W. Oo, A. Pizzi, A. Trosa, M.F. Thevenon, Metal adsorption of tannin based rigid foams, Ind. Crop. Prod., 29 (2009) 336–340.
[13] J. Sánchez-Martín, J. Beltrán-Heredia, A. Delgado-Regaña, M.A. Rodríguez-González, F. Rubio-Alonso, Adsorbent tannin foams: new and complementary applications in wastewater treatment, Chem. Eng. J., 228 (2013) 575–582.
[14] C. Lacoste, M.C. Basso, A. Pizzi, M.P. Laborie, A. Celzard, V. Fierro, Pine tannin-based rigid foams: mechanical and thermal properties, Ind. Crop. Prod., 43 (2013) 245–250.
[15] C. Li, R. Leverence, J.D. Trombley, S. Xu, J. Yang, Y. Tian, High molecular weight persimmon (*Diospyros kaki* L.) proanthocyanidin: a highly galloylated, A-linked tannin with an unusual flavonol terminal unit, myricetin, J. Agric. Food. Chem., 58 (2010) 9033–9042.
[16] R. Fan, F. Xie, X. Guan, Q. Zhang, Z. Luo, Selective adsorption and recovery of Au(III) from three kinds of acidic systems by persimmon residual based bio-sorbent: a method for gold recycling from e-wastes, Bioresour. Technol., 163 (2014) 167–171.
[17] X. Huang, Y. Wang, X. Liao, B. Shi, Adsorptive recovery of Au^{3+} from aqueous solutions using bayberry tannin-immobilized mesoporous silica, J. Hazard. Mater., 183 (2010) 793–798.
[18] S.J. Allen, G. McKay, K.Y.H. Khader, Intraparticle diffusion of a basic dye during adsorption onto sphagnum peat, Environ. Pollut., 56 (1989) 39–50.
[19] M. Soleimani, T. Kaghazchi, Adsorption of gold ions from industrial wastewater using activated carbon derived from hard shell of apricot stones – an agricultural waste, Bioresour. Technol., 99 (2008) 5374–5383.
[20] L. Sun, C. Tian, L. Wang, J. Zou, G. Mu, H. Fu, Magnetically separable porous graphitic carbon with large surface area as excellent adsorbents for metal ions and dye, J. Mater. Chem., 21 (2011) 7232.
[21] A.B. Farag, M.H. Soliman, O.S. Abdel-Rasoul, M.S. el-Shahawi, Sorption characteristics and chromatographic separation of gold (I and III) from silver and base metal ions using polyurethane foams, Anal. Chim. Acta., 601 (2007) 218–229.
[22] M. Matsumoto, D. Kawabata, T. Takatani, Y. Yoshida, K. Kondo, Selective adsorption of oxometallic and gold ions on filter paper containing cedar bark, Solvent Extr. Ion. Exc., 32 (2013) 111–118.

[23] S. Aktas, M.H. Morcali, Gold uptake from dilute chloride solutions by a Lewatit TP 214 and activated rice husk, Int. J. Miner. Process., 101 (2011) 63–70.

[24] R. Chand, T. Watari, K. Inoue, H. Kawakita, H.N. Luitel, D. Parajuli, Selective adsorption of precious metals from hydrochloric acid solutions using porous carbon prepared from barley straw and rice husk, Miner. Eng., 22 (2009) 1277–1282.

[25] M.R. Awual, M.A. Khaleque, M. Ferdows, A.M.S. Chowdhury, T. Yaita, Rapid recognition and recovery of gold(III) with functional ligand immobilized novel mesoporous adsorbent, Microchem. J., 110 (2013) 591–598.

[26] K.F. Lam, C.M. Fong, K.L. Yeung, G. McKay, Selective adsorption of gold from complex mixtures using mesoporous adsorbents, Chem. Eng. J., 145 (2008) 185–195.

[27] T. Matsuo, S. Ito, The chemical structure of kaki-tannin from immature fruit of the persimmon (*Diospyros kaki* L.), Agric. Biol. Chem., 42 (1978) 1637–1643.

Supplementary material

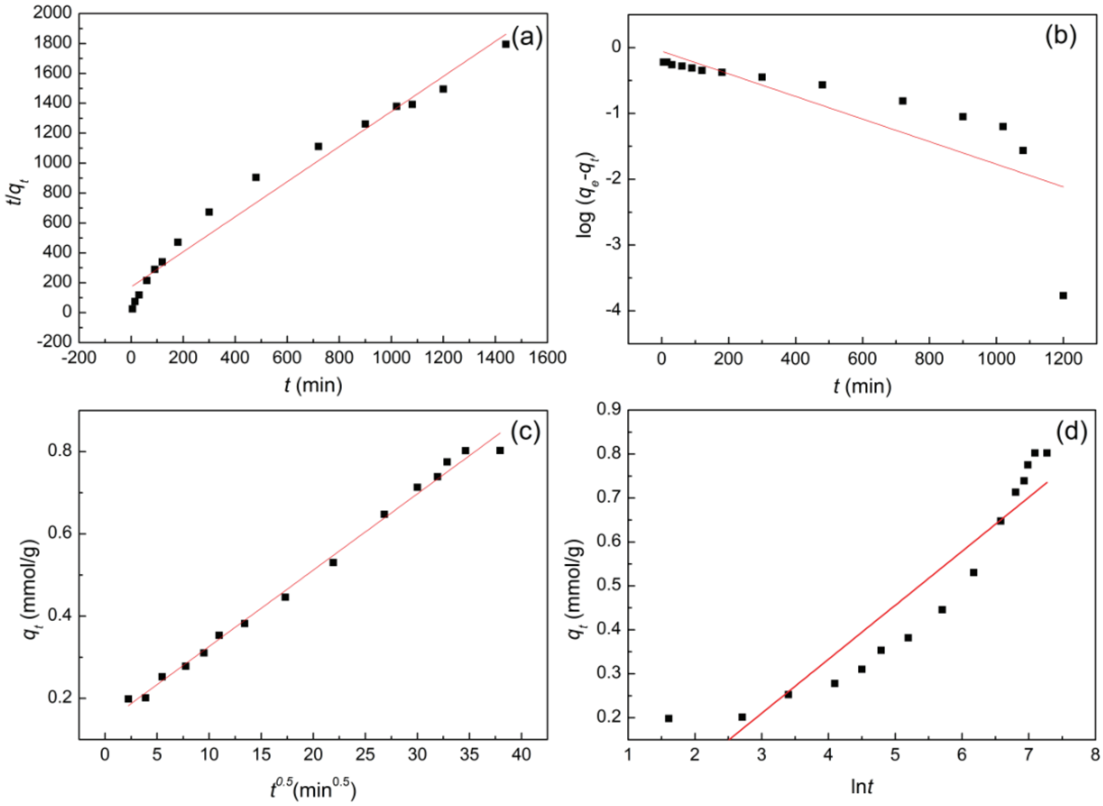

Fig. S1. Pseudo-first-order (a), Pseudo-second-order (b), Intraparticle diffusion (c) and Elovich (d) kinetic plots of the adsorption of Kaki-TRF on Au(Ⅲ). (q_e: equilibrium adsorption amount; q_t: adsorption amount at time *t*).

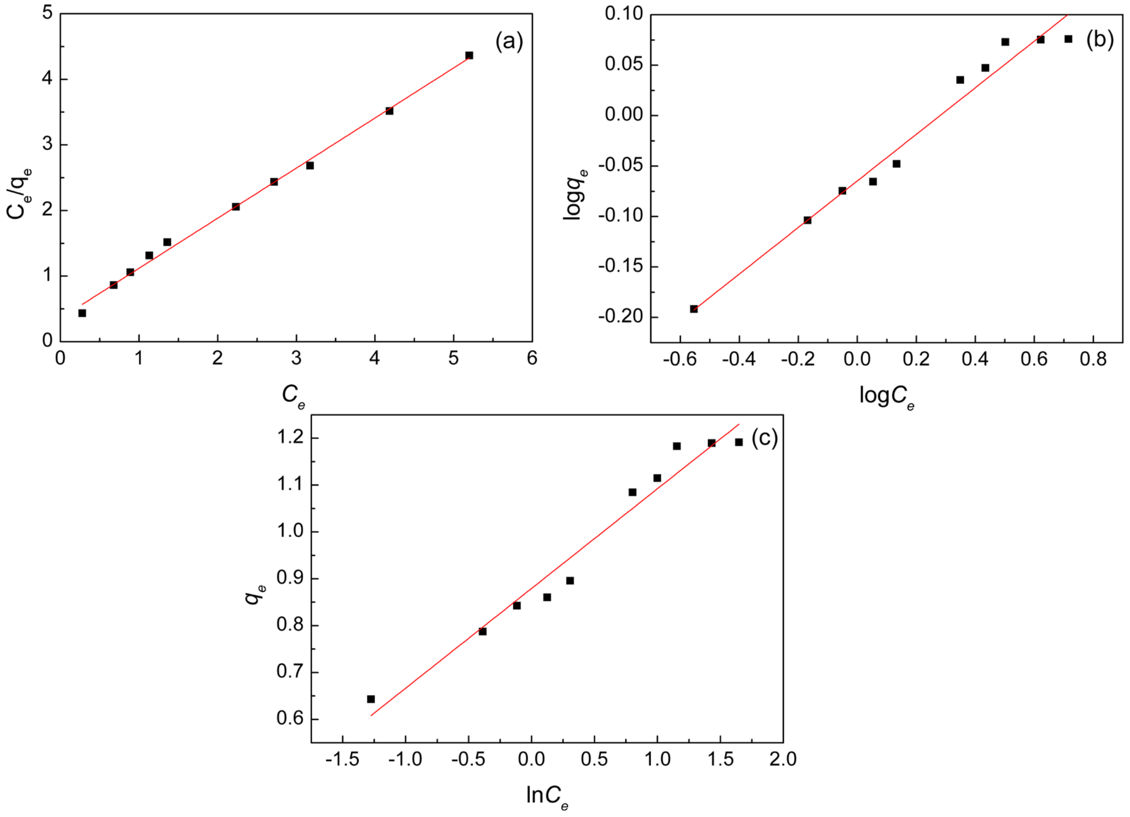

Fig. S2. Langmuir (a), Freundlich (b) and Temkin (c) isotherm plots of the adsorption of Kaki-TRF on Au(Ⅲ). (q_e: equilibrium adsorption amount; C_e: conc. of Au(Ⅲ) at equilibrium).

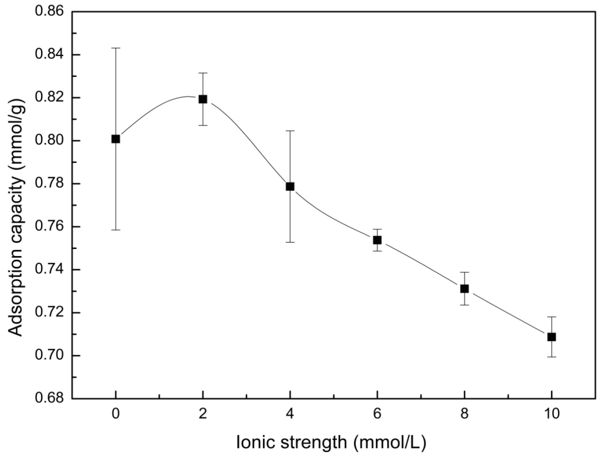

Fig. S3. Effect of ionic strength on Au(Ⅲ) adsorption capacity. (Weight of adsorbent = 15 mg, volume of Au(Ⅲ)-solution = 20 mL, concentration of Au(Ⅲ) = 1 mM, temperature = 25°C, shaking time = 24 h, shaking speed = 180 rpm).